K^+ Activation of Kir3.1/Kir3.4 and Kv1.4 K^+ Channels Is Regulated by Extracellular Charges

T. W. Claydon, S. Y. Makary, K. M. Dibb, and M. R. Boyett
School of Biomedical Sciences, University of Leeds, Leeds, United Kingdom

ABSTRACT K^+ activates many inward rectifier and voltage-gated K^+ channels. In each case, an increase in K^+ current through the channel can occur despite a reduced driving force. We have investigated the molecular mechanism of K^+ activation of the inward rectifier K^+ channel, Kir3.1/Kir3.4, and the voltage-gated K^+ channel, Kv1.4. In the Kir3.1/Kir3.4 channel, mutation of an extracellular arginine residue, R155, in the Kir3.4 subunit markedly reduced K^+ activation of the channel. The same mutation also abolished Mg^{2+} block of the channel. Mutation of the equivalent residue in Kv1.4 (K532) abolished K^+ activation as well as C-type inactivation of the Kv1.4 channel. Thus, whereas C-type inactivation is a collapse of the selectivity filter, K^+ activation could be an opening of the selectivity filter. K^+ activation of the Kv1.4 channel was enhanced by acidic pH. Mutation of an extracellular histidine residue, H508, that mediates the inhibitory effect of protons on Kv1.4 current, abolished both K^+ activation and the enhancement of K^+ activation at acidic pH. These results suggest that the extracellular positive charges in both the Kir3.1/Kir3.4 and the Kv1.4 channels act as "guards" and regulate access of K^+ to the selectivity filter and, thus, the open probability of the selectivity filter. Furthermore, these data suggest that, at acidic pH, protonation of H508 inhibits current through the Kv1.4 channel by decreasing K^+ access to the selectivity filter, thus favoring the collapse of the selectivity filter.

INTRODUCTION

Almost 40 years ago, McAllister and Noble (1966) showed that extracellular K^+ activates the cardiac inward rectifier K^+ current, $I_{K,1}$. Both the inward and outward components of $I_{K,1}$ are enhanced in high extracellular K^+, leading to the so-called ''crossover'' effect. More recently, Kubo et al. (1996) showed that current through the Kir2.1 inward rectifier (Kir) K^+ channel, which underlies $I_{K,1}$ (Zobel et al., 2003), is also activated by extracellular K^+. All Kir subunits, with the exception of Kir7.1, have a positively charged arginine residue close to the extracellular mouth of the selectivity filter (at position +2 with respect to the GYG sequence; Fig. 1 *C*). The Kir7.1 channel shows an increased Rb^+ conductance and is not activated by extracellular K^+, unlike the other Kir channels. Introduction of the arginine residue not only reduces Rb^+ conductance, it also introduces K^+ activation (Doring et al., 1998; Wischmeyer et al., 2000). The arginine residue could, therefore, be responsible for K^+ activation in the other Kir channels, and in particular the cardiac Kir3.1/Kir3.4 channel, and one aim of our study was to test this.

K^+ activation occurs in a number of voltage-gated (Kv) K^+ channels, including the Kv1.3 and Kv1.4 (Pardo et al., 1992), *Shaker* (Lopez-Barneo et al., 1993; Baukrowitz and Yellen, 1995), and Kv2.1 (Wood and Korn, 2000) channels. In Kv channels, K^+ activation is thought to be the result of an increased number of available channels, because neither the single-channel conductance nor mean open time of the Kv1.4 channel is altered in high extracellular K^+ (Pardo et al., 1992). This possibility is consistent with studies on the *Shaker* channel, which show that increased extracellular K^+ slows or abolishes C-type inactivation (Lopez-Barneo et al., 1993; Baukrowitz and Yellen, 1995). The fact that the permeant ion can slow C-type inactivation suggests that a modulatory site (perhaps a K^+ coordination site in the selectivity filter) must be emptied of K^+ before C-type inactivation can occur—in high extracellular K^+, this site is more likely to be filled by K^+ so that C-type inactivation is less likely to occur (Lopez-Barneo et al., 1993). The residue at position 449 in the *Shaker* channel is important in determining C-type inactivation and therefore may determine K^+ occupancy of the modulatory site (Lopez-Barneo et al., 1993; Ogielska and Aldrich, 1999). In the Kv1.4 channel, the equivalent residue is lysine 532 (K532), which is at position +3 with respect to the GYG sequence (Fig. 1 *C*). There is some evidence, although not conclusive, that this residue is involved in K^+ activation of the Kv1.4 channel (Pardo et al., 1992). Recently, we have shown that K532, along with H508, is responsible for pH modulation of C-type inactivation of the Kv1.4 channel (Claydon et al., 2002). This raises the possibility that there is an interaction between pH and K^+ activation, and so we have investigated the involvement of K532, H508, and pH in K^+ activation of the cardiac Kv1.4 channel.

In this study, we have obtained evidence that the positively charged arginine residue in the Kir3.1/Kir3.4 channel regulates access of K^+ to the selectivity filter and, thus, K^+ activation. We show evidence of a similar role for the positively charged lysine residue in the Kv1.4 channel. We show evidence that the positively charged residue, H508, in the Kv1.4 channel also regulates K^+ access to the selectivity filter and, thus, K^+ activation. Finally, we show in the Kv1.4 channel that K^+ activation is enhanced at acidic pH and that

Submitted December 23, 2003, and accepted for publication July 13, 2004.

Address reprint requests to M. R. Boyett, School of Biomedical Sciences, University of Leeds, Leeds LS2 9JT, UK. Tel.: 44-113-3434298; Fax: 44-113-3434224; E-mail: m.r.boyett@leeds.ac.uk.

0006-3495/04/10/2407/12 $2.00

doi: 10.1529/biophysj.103.039073

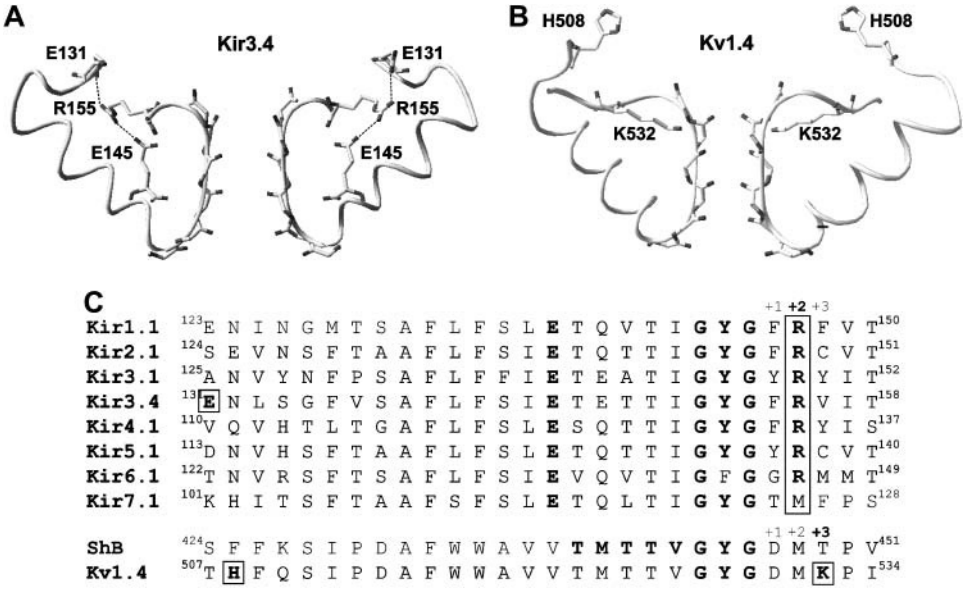

FIGURE 1 (*A*) Comparative model of the outer pore region of the Kir3.1/Kir3.4 channel based on the structure of the KcsA channel. The two Kir3.1 subunits have been removed for clarity. The R155, E145, and E131 residues and the carbonyl oxygen atoms of the selectivity filter are highlighted. The salt bridges between R155 and E145 and E131 residues are shown by the dashed lines. (*B*) Comparative model of the outer pore region of the Kv1.4 channel based on the structure of the KcsA channel. Two subunits have been removed for clarity. The K532 and H508 residues and the carbonyl oxygen atoms of the selectivity filter are highlighted. (*C*) Sequence alignment of the Kir channel family members (*top*) and *Shaker* (*ShB*) and Kv1.4 (*bottom*). The arginine residues equivalent to R155 in Kir3.4 and K532 in Kv1.4 are highlighted by the boxes as well as E131 in Kir3.4 and H508 in Kv1.4. The GYG motif and the glutamate residues equivalent to E145 in Kir3.4 (which form a salt bridge with the highlighted arginine residues) are also highlighted in bold.

this is abolished by mutation of K532 or H508. These data suggest that positive charges at the extracellular end of the pores of both Kir and Kv channels determine K^+ occupancy within the selectivity filter and, thus, K^+ activation.

MATERIALS AND METHODS

Molecular biology

Experiments were performed on wild-type or mutant forms of the Kir3.1/Kir3.4 or Kv1.4 K^+ channels. Mutations were made and cRNA transcribed as previously described (Claydon et al., 2000, 2002).

Electrophysiology

Xenopus oocytes were isolated and prepared as described previously (Claydon et al., 2000). Oocytes were injected with 50 nl cRNA encoding wild-type or mutant Kir3.1 (30 ng/μl) and Kir3.4 (30 ng/μl) or wild-type or mutant Kv1.4 (50 ng/μl). In the case of the Kir3.1/Kir3.4 channel, hD2 (human dopamine receptor) was also injected (3.8 ng/μl), as this was required to activate the channel. Oocytes were incubated in Barth's medium (in mM): 88 NaCl, 1 KCl, 2.4 $NaHCO_3$, 0.82 $MgSO_4$, 0.33 $Ca(NO_3)_2$, 0.41 $CaCl_2$, 1.25 sodium pyruvate, 0.1 mg/ml neomycin (Sigma, Poole, UK), 100 units/0.1 mg/ml penicillin/streptomycin mix (Sigma), 20 HEPES, pH 7.4 (with NaOH). Currents were recorded 16–72 h later using the two-electrode voltage clamp technique using a Geneclamp 500B amplifier filtering at 500 Hz and sampling at 2 kHz (Axon Instruments, Union City, CA). Electrodes were filled with 3 M KCl (tip resistance, 1–3 MΩ). Experiments were performed at 20–22°C. To measure current-voltage relationships, current was recorded during 750 ms voltage-clamp pulses from −130 to +60 mV from a holding potential of 0 mV (pulse frequency, 0.33 Hz) in the case of the Kir3.1/Kir3.4 channel, and during 200-ms voltage-clamp pulses from −80 to +90 mV from a holding potential of −80 mV (pulse frequency, 0.5 Hz) in the case of the Kv1.4 channel. To measure recovery of the Kv1.4 channel from inactivation, currents were recorded during a 200-ms test pulse to +40 mV at different intervals after a 200-ms conditioning pulse to +40 mV (holding potential −80 mV, pulse frequency 0.067 Hz). In the case of the Kir3.1/Kir3.4 channel, K^+ activation was measured by recording currents initially during perfusion of solution containing 9 mM KCl (in mM: 9 KCl, 81 NMDG (*N*-methyl-D-glucamine), 2 $CaCl_2$, 5 HEPES, pH 7.4, with KOH) and then with solution containing 27, 45, or 90 mM KCl (equimolar substitution of NMDG). To measure the effect of extracellular Mg^{2+}, 1, 3, 10, or 30 mM $MgCl_2$ was added to the 90 mM KCl solution. In the case of the Kv1.4 channel, oocytes were perfused initially with ND96 solution (in mM: 96 NaCl, 3 KCl, 2 $CaCl_2$, 5 HEPES, pH 7.4, with NaOH), to obtain control current recordings. To measure K^+ activation of the Kv1.4 channel, solution in which the NaCl had been replaced with KCl (final KCl concentration, 99 mM) was applied. In all cases, solution was perfused at a flow rate of ~5 ml/min (bath volume, ~100 μl) and 30 s was allowed for a steady state to be achieved before current was recorded.

Analysis and statistics

Data were analyzed using pClamp software (Axon Instruments) and are shown as mean ± SEM (number of oocytes). Chord and slope conductance was calculated from current-voltage relationships. Mean chord conductance values at E_K could be calculated because the reversal potential was not always zero. Slope conductance was calculated using a linear regression of data between −130 and −110 mV. Dose response curves for Mg^{2+} block were fitted with the equation:

$$y = 1 - ([Mg^{2+}]^n/(K_D^n + [Mg^{2+}]^n), \quad (1)$$

where y is the fractional current remaining in the presence of Mg^{2+}, $[Mg^{2+}]$ is the extracellular concentration of Mg^{2+}, K_D is the dissociation constant, and n is the Hill coefficient. K_D was plotted against the membrane potential, V, and fitted with the equation

$$K_D = K_D(0)\exp(\delta zVF/RT), \quad (2)$$

where $K_D(0)$ is the dissociation constant at 0 mV, δ is the fraction of the electrical field experienced by the blocking ion at its binding site, and z, F, R,

and *T* have their usual meanings. Statistical analysis was carried out using Student's *t*-test or one-way analysis of variance (ANOVA) as appropriate using SigmaStat (SPSS Science, Chicago, IL). *P* values of <0.05 were assumed to indicate a significant difference.

Modeling

Comparative models of the Kir3.1/Kir3.4 and Kv1.4 channels were constructed based on the crystal structure of KcsA as described previously (Claydon et al., 2000; Dibb et al., 2003). Models of amino acid side-chain rotamer positions were calculated using Swiss-Pdb Viewer (Guex and Peitsch, 1997). Rotamers were scored according to clashes with other backbone and side-chain atoms. The rotamer with the lowest score was considered the ''best'' rotamer.

RESULTS

K^+ activation of the Kir3.1/Kir3.4 channel is mediated by an extracellular positive charge

Fig. 1 *C* shows an alignment of the outer pore region, including the selectivity filter, of all known Kir subunits. All Kir subunits, with the exception of Kir7.1, possess a positively charged arginine residue (highlighted) at +2 residues from the GYG motif. We have investigated the role of this arginine residue in K^+ activation of the Kir3.1/Kir3.4 channel. In Kir3.1, the arginine residue is at position 149, and in Kir3.4 it is at position 155. A comparative model of the outer pore and selectivity filter of the Kir3.1/Kir3.4 channel is shown in Fig. 1 *A*. Only the two Kir3.4 subunits are shown for clarity; the two Kir3.1 subunits have been removed. The R155 residue (and E131 and E145 residues; see below) of Kir3.4 and the carbonyl oxygen atoms that coordinate K^+ in the selectivity filter are highlighted.

Fig. 2 shows the effect of raising extracellular K^+ on current through wild-type and mutant forms of the Kir3.1/Kir3.4 channel. Typical current traces recorded during 750 ms voltage-clamp pulses to −130 mV from a holding potential of 0 mV in either 9 or 90 mM extracellular K^+ are shown in Fig. 2 *A*. The wild-type Kir3.1/Kir3.4 channel was significantly activated by raising K^+; current at −130 mV was −5.1 ± 1.1 and −30.5 ± 6.3 mA ($n = 5$) in 9 and 90 mM K^+, respectively. This is also shown by the mean current-voltage relationships and conductance-voltage relationships, recorded with a number of K^+ concentrations, in panels *B* and *C*, respectively, of Fig. 2. Raising extracellular K^+ from 9 to 90 mM caused a 6.1 ± 0.3-fold increase in current and a 4.1 ± 0.3-fold increase in conductance through the wild-type Kir3.1/Kir3.4 channel at −130 mV. The increase in conductance on raising extracellular K^+ (Fig. 2 *C*) is defined as K^+ activation of the Kir3.1/Kir3.4 channel.

Due to small current amplitude, it was not possible to study the effect of extracellular K^+ with the Kir3.1[R149E]/Kir3.4[R155E] mutant channel. However, current through Kir3.1/Kir3.4[R155E] and Kir3.1/Kir3.4[R155Q] mutant channels was large enough to measure accurately. Although current through both mutant channels was still increased by raising extracellular K^+, the effect was markedly reduced (Fig. 2, *A–C*). Current at −130 mV was −2.3 ± 0.4 and −5.7 ± 1.1 mA and −3.1 ± 0.7 and −7.5 ± 0.8 mA in 9 and 90 mM K^+ in the Kir3.1/Kir3.4[R155E] and Kir3.1/Kir3.4[R155Q] mutant channels, respectively ($n = 5$–6). This corresponds to a 1.7 ± 0.2- and 2.2 ± 0.2-fold increase in conductance, respectively, and is significantly different

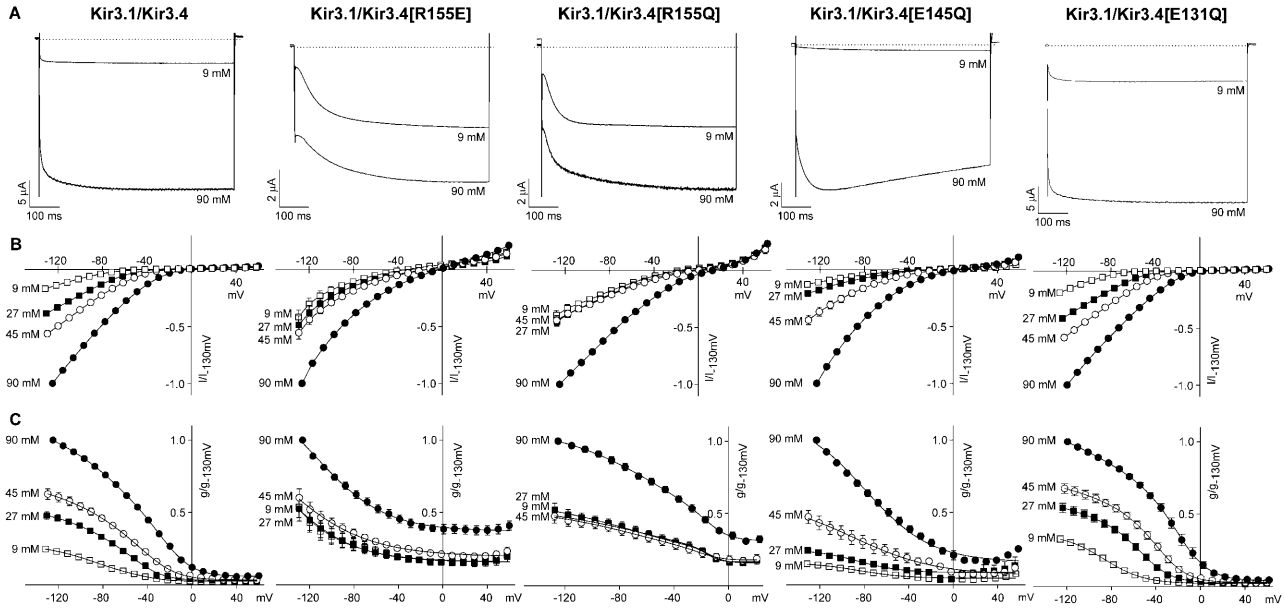

FIGURE 2 K^+ activation of wild-type and mutant Kir3.1/Kir3.4 channels. (*A*) Typical current traces recorded during 750-ms voltage pulses to −130 mV from a holding potential of 0 mV in 9 and 90 mM K^+. The dotted line marks zero current. (*B* and *C*) Current-voltage relationships (*B*) and conductance-voltage relationships (*C*) for each channel in a range of K^+ concentrations. Mean ± SEM ($n = 5$) shown. Currents are normalized to the current at −130 mV in 90 mM K^+. Conductance values are normalized to the conductance at −130 mV in 90 mM K^+.

from the 4.1 ± 0.3-fold increase in the wild-type Kir3.1/Kir3.4 channel (ANOVA, $P < 0.05$).

Yang et al. (1997) showed that the equivalent residue to R155 in the Kir2.1 channel, R148, forms a salt bridge behind the selectivity filter with a negatively charged glutamate residue, E138. We have recently shown (Dibb et al., 2003) that a similar salt bridge exists in the Kir3.1/Kir3.4 channel between R155 and E145, and that R155 may also interact with E131 in the extracellular loop (Fig. 1, *A* and *C*). Disruption of the salt bridge between R155 and E145 by neutralization or reversal of either charge results in increased flexibility of the selectivity filter and loss of ion selectivity (Dibb et al., 2003). The effects of disruption of the interaction between R155 and E131 are unknown. To test whether the reduction in K^+ activation caused by mutation of R155 was the result of disruption of the salt bridges, we also measured K^+ activation in Kir3.1/Kir3.4[E145Q] and Kir3.1/Kir3.4[E131Q] mutant channels. Fig. 2 shows that disruption of either salt bridge, while retaining R155, had modest effects on K^+ activation.

These data are summarized in Fig. 3 by plots of conductance against K^+ concentration: Fig. 3 *A* shows chord conductance and Fig. 3 *B* shows slope conductance (both forms of conductance calculation give similar results). These data show that K^+ activation of the Kir3.1/Kir3.4 channel was markedly reduced by mutation of R155. K^+ activation was also reduced by mutation of E131, but to a smaller extent than mutation of R155. Mutation of E145 did not reduce K^+ activation (although the mutation of E145 shifted the relationship). This suggests that mutation of R155 does not alter K^+ activation by disrupting the salt bridges and that the R155 residue itself is important for K^+ activation.

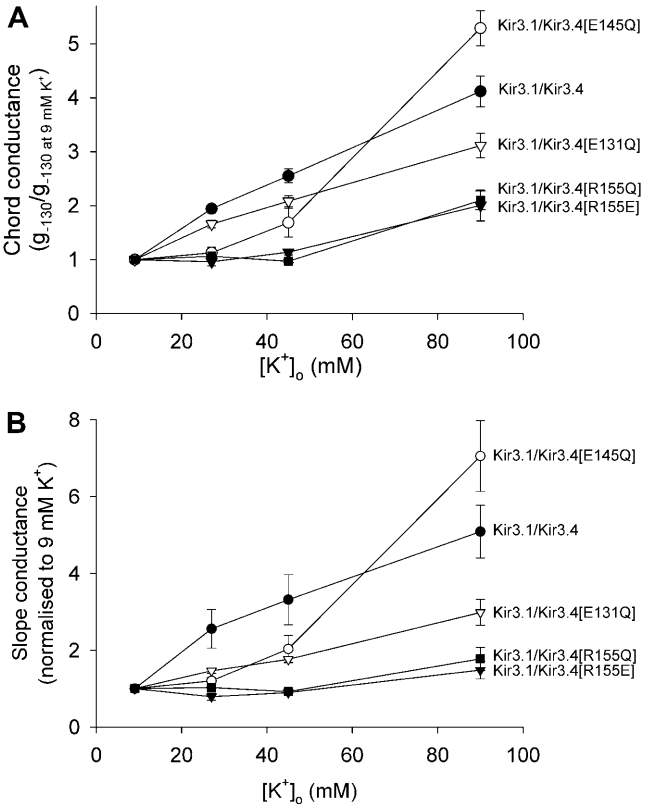

FIGURE 3 Summary of K^+ activation. (*A*) Chord conductance at −130 mV plotted against K^+ concentration for the different channels. (*B*) Slope conductance, calculated using a linear regression of data from −130 to −110 mV, plotted against K^+ concentration for the different channels. Conductance is normalized to that at 9 mM K^+. Lines are to guide the eye. Mean ± SEM ($n = 5$) shown.

Mutation of R155 also alters Mg^{2+} access to the Kir3.1/Kir3.4 pore

If the salt bridge between R155 and E145 is broken, blocking ions such as Cs^+ and Ba^{2+} no longer block and instead permeate the channel, because of the increased flexibility of the selectivity filter (Dibb et al., 2003). However, Fig. 4 shows that Mg^{2+} access to the pore is restricted even if this salt bridge is broken. Fig. 4 *A* shows typical currents recorded from wild-type and mutant Kir3.1/Kir3.4 channels during 750-ms voltage-clamp pulses from −130 to +40 mV from a holding potential of 0 mV in the absence and presence of 10 mM Mg^{2+}. Mg^{2+} blocked the wild-type Kir3.1/Kir3.4 channel. This is shown clearly by the mean current-voltage relationships recorded with a range of Mg^{2+} concentrations in Fig. 4 *B*. From these data, dose-response curves (Fig. 5 *A*) were plotted. The dissociation constant, K_D, at −130 mV was 3.7 ± 0.4 mM ($n = 7$). Fig. 5 *B* shows that the K_D of Mg^{2+} block varied with voltage. From this, δ, the fraction of the electrical field that Mg^{2+} must cross to reach its blocking site, was calculated to be 0.18. Surprisingly, whereas disruption of the salt bridge by the mutation, E145Q, abolishes block by monovalent and divalent cations (Cs^+ and Ba^{2+}; Dibb et al., 2003), Mg^{2+} block of the channel remained (Figs. 4 and 5); at −130 mV, the K_D was 4.9 ± 0.5 mM ($n = 14$, ANOVA not significantly different from the wild-type channel, however, δ was reduced to 0.0004, Fig. 5 *B*). In contrast, the mutation, R155E, abolished Mg^{2+} block of the channel (Figs. 4 and 5). Current through the Kir3.1/Kir3.4[R155E] channel was not reduced in the presence of Mg^{2+} (Fig. 4) and was actually increased in the presence of 30 mM Mg^{2+} (Fig. 4 *B*), suggesting that Mg^{2+} now permeated the channel. In contrast to the striking effect of the R155E mutation, replacement of the positive charge with a neutral glutamine, R155Q, only reduced Mg^{2+} block to a small extent (Fig. 5). Recently, Murata et al. (2002) showed that the equivalent residue to E131 in the Kir2.1 channel, E125 (see Fig. 1 *C*), is involved in block by extracellular Mg^{2+}. Figs. 4 and 5 show that the E131Q mutation in the Kir3.1/Kir3.4 channel also reduced Mg^{2+} block. Clearly, E131 is important for Mg^{2+} block of the Kir3.1/Kir3.4 channel; however, the abolition of Mg^{2+} block and evidence of Mg^{2+} permeation on replacement of R155 with a negative charge (Figs. 4 and 5) suggests that the charge at this position is also important.

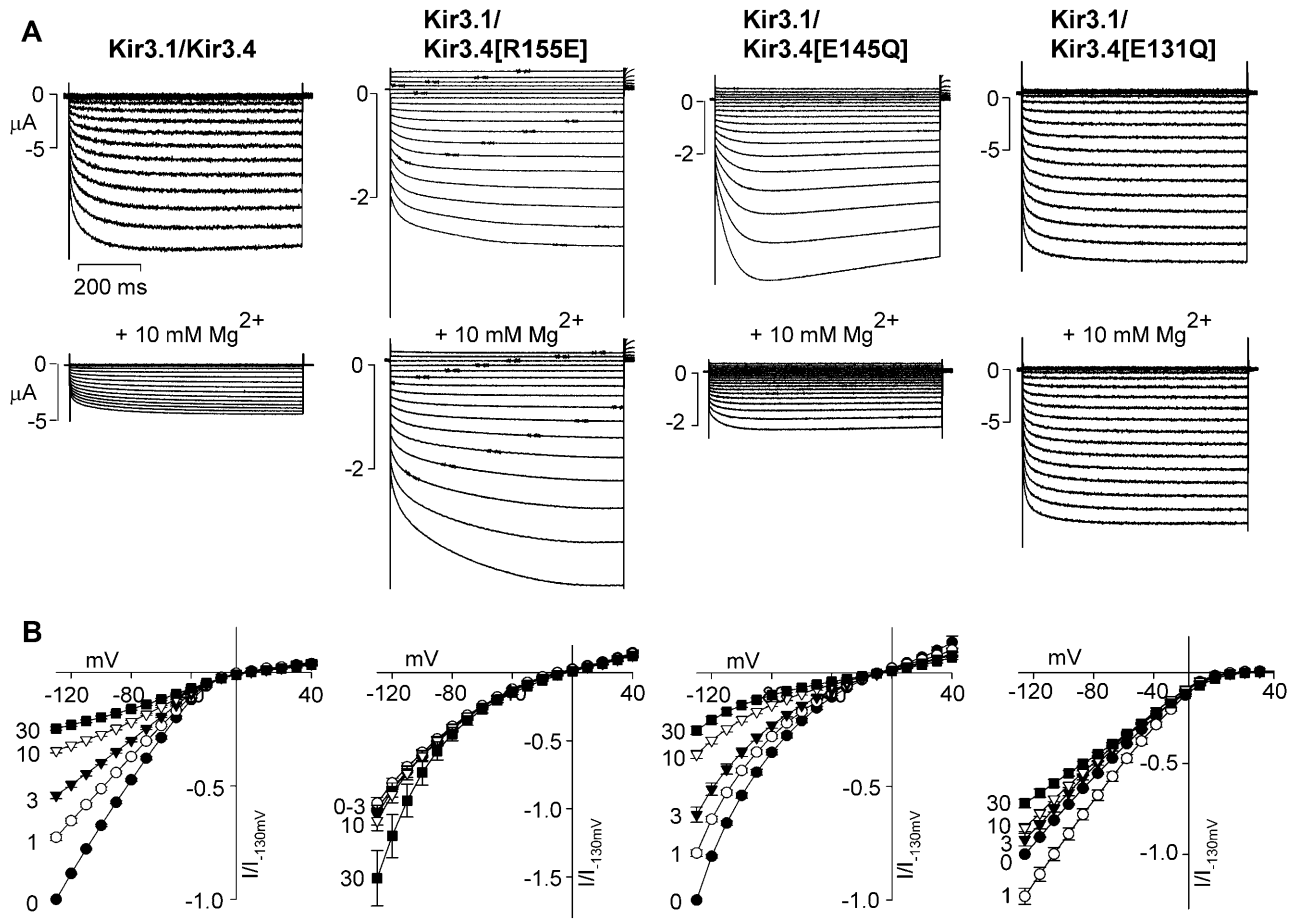

FIGURE 4 Mg^{2+} block of wild-type and mutant Kir3.1/Kir3.4 channels. (*A*) Typical current traces recorded during voltage pulses from −130 to +40 mV from a holding potential of 0 mV in the absence and presence of 10 mM Mg^{2+}. (*B*) Current-voltage relationships for each channel tested with a range of Mg^{2+} concentrations. Mean ± SEM ($n = 5$) shown. Currents are normalized to the current at −130 mV in the absence of Mg^{2+}.

Extracellular positive charges also regulate K^+ activation of the Kv1.4 channel

The data in Fig. 2 suggest that R155 in the Kir3.1/Kir3.4 channel is responsible for K^+ activation. Fig. 1 *C* shows an alignment of the outer pore region of the Kv1.4 channel with the *Shaker* channel. Kv1.4 has a positively charged lysine residue (K532, *highlighted*) at a similar position to R155 in Kir3.4. K532 in Kv1.4 lies +3 residues from the GYG motif. We therefore investigated the role of K532 in K^+ activation of the Kv1.4 channel.

Fig. 6 shows the effect of raising extracellular K^+ on current through wild-type and mutant Kv1.4 channels. Typical current traces recorded during perfusion of either 3 or 99 mM extracellular K^+ are shown in Fig. 6 *A*. Currents were recorded during 200-ms voltage-clamp pulses to +90 mV from a holding potential of −80 mV. Despite the reduction in driving force, raising extracellular K^+ from 3 to 99 mM increased current through the wild-type Kv1.4 channel; peak current minus current at the end of the pulse at +90 mV was 5.2 ± 1.0 and 10.6 ± 1.3 mA in 3 and 99 mM K^+, respectively ($n = 4$; paired *t*-test, $P < 0.001$). Current amplitude was increased 2.2 ± 0.2-fold ($n = 4$). This increase in current through the channel is also shown by the mean current-voltage relationships in Fig. 6 *B*. From these data, conductance-voltage relationships were calculated (Fig. 6 *C*). At +90 mV, raising extracellular K^+ from 3 to 99 mM increased wild-type Kv1.4 conductance 3.4 ± 0.3-fold.

Fig. 1 *B* shows a comparative model of the outer pore region of the Kv1.4 channel based on the structure of the KcsA channel (Zhou et al., 2001). Only two subunits are shown for clarity. K532, H508, and the carbonyl oxygen atoms that coordinate K^+ in the selectivity filter are highlighted. We have previously shown that K532 and H508 are responsible for pH regulation of the channel (Claydon et al., 2000, 2002). Fig. 6 shows that either the mutation, K532Y, or the mutation, H508Q, abolished K^+ activation. In both mutant channels, current was little affected by raising extracellular K^+ from 3 to 99 mM K^+ (Fig. 6 *A*). In the case of the K532Y mutant channel, peak minus end current at +90 mV was 9.2 ± 3.1 and 10.8 ± 2.3 mA in 3 and 99 mM K^+, respectively ($n = 4$; paired *t*-test, not significantly different), and in the case of the H508Q

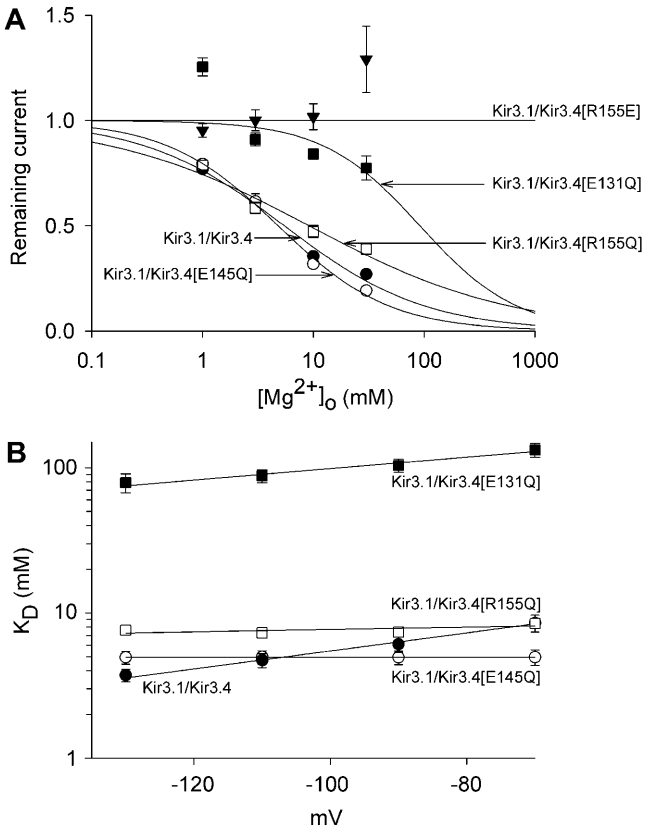

FIGURE 5 Dose-response curves (*A*) and plots of the dissociation constant against membrane potential (*B*) for Mg^{2+} block of wild-type and mutant Kir3.1/Kir3.4 channels. In *A*, dose-response curves at −130 mV are shown for Mg^{2+} block of each channel tested. Data (with the exception of the Kir3.1/Kir3.4[R155E] data) were fitted with Eq. 1. The Hill coefficient, *n*, was 0.7, 0.9, 0.5, and 1.0 for Kir3.1/Kir3.4, Kir3.1/Kir3.4[E145Q], Kir3.1/Kir3.4[R155Q], and Kir3.1/Kir3.4[E131Q], respectively. In *B*, the dissociation constant, K_D, is plotted against the membrane potential for the wild-type and mutant channels. Data were fitted with Eq. 2. Mean ± SEM ($n = 5$) shown.

mutant channel, peak minus end current at +90 mV was 8.1 ± 2.7 and 11.4 ± 4.1 mA in 3 and 99 mM K^+, respectively ($n = 5$; paired *t*-test, not significantly different). This is also shown by the mean current-voltage relationships in Fig. 6 *B*. The conductance-voltage relationships in Fig. 6 *C* show that the increase in conductance associated with raising extracellular K^+ was reduced by ~50% by each mutation. Pardo et al. (1992) previously showed that the double mutation K532Y, I534M abolishes K^+ activation of the Kv1.4 channel. To confirm the role of K532 suggested by the experiments in Fig. 6, we investigated the effect of the mutation I534M on K^+ activation (Fig. 6). The I534M mutation did not abolish, but instead enhanced, K^+ activation. These data show that neutralization of the K532 or H508 charges alters K^+ activation of the Kv1.4 channel.

Acidic pH enhances K^+ activation of the Kv1.4 channel

Fig. 7 shows that K^+ activation of current through the wild-type Kv1.4 channel was enhanced at low pH. Fig. 7 *A* (*left*) shows typical wild-type Kv1.4 currents recorded at +90 mV in 3 and 99 mM K^+ at either pH 7.4 or pH 6.5. The increase in current with 99 mM K^+ was enhanced at pH 6.5. Current at +90 mV was 4.5 ± 1.1-fold larger in 99 mM K^+ than in 3 mM K^+ at pH 6.5 compared with 2.2 ± 0.2-fold larger at pH 7.4 ($n = 4$; paired *t*-test, $P < 0.05$). This is also shown by the mean current-voltage relationships in Fig. 7 *B* (*left*), which show current in 99 mM K^+ normalized to that in 3 mM K^+ at either pH 7.4 or pH 6.5. Conductance-voltage relationships (Fig. 7 *C*) calculated from these data show that, at pH 6.5, conductance at +90 mV was increased 5.3 ± 1.2-fold by raising extracellular K^+ from 3 to 99 mM compared with a 3.4 ± 0.3-fold increase at pH 7.4.

The extracellular histidine residue, H508, shown in Fig. 6 to be important in mediating K^+ activation of the Kv1.4 channel, has previously been shown to be involved with the inhibitory effect of acidic pH on current through the Kv1.4 channel (Claydon et al., 2000, 2002). Here we show that neutralization of H508, by the mutation H508Q, also abolished the effect of acidic pH on K^+ activation of current through the Kv1.4 channel. Fig. 7 *A* (*right*) shows that at +90 mV current through the H508Q mutant channel was not enhanced in 99 mM K^+ at pH 6.5. The mean current-voltage relationships in Fig. 7 *B* (*right*) show that, at +90 mV, current in 99 mM K^+ was 1.5 ± 0.1 times the size of current in 3 mM K^+ at pH 7.4 and 1.5 ± 0.3 times the size of current in 3 mM K^+ at pH 6.5 ($n = 5$; ANOVA, not significantly different). The conductance-voltage relationships in Fig. 7 *C* (*right*) confirm that acidic pH did not enhance the effect of extracellular K^+ on the H508Q mutant channel as it does in the wild-type Kv1.4 channel.

Regulation of Kv1.4 K^+ activation by regulation of C-type inactivation

Baukrowitz and Yellen (1995) showed that K^+ activation of the *Shaker* channel requires both C-type and N-type inactivation mechanisms. Fig. 8 *A* shows the time course of recovery from inactivation of wild-type and mutant Kv1.4 channels in 3 and 99 mM K^+. This is known to be governed by recovery from C-type inactivation (Rasmusson et al., 1995). Recovery of wild-type Kv1.4 from inactivation occurred with a time constant, τ, of 1968 ± 491 ms in 3 mM K^+ and this was reduced to 125 ± 35 ms in 99 mM K^+ ($n = 4$). The data shown in Figs. 5 and 6 were obtained with a pulse interval of 2 s, which is represented by the vertical dashed line in Fig. 8 *A*. At a pulse interval of 2 s, recovery of the wild-type Kv1.4 channel from inactivation was complete at 99 mM K^+, but not at 3 mM K^+ (Fig. 8 *A*). With a 2-s interval, the incomplete recovery in 3 mM K^+ and the complete recovery in 99 mM K^+ explains the increase of wild-type Kv1.4 current during repetitive pulsing on going from 3 to 99 mM K^+ (Figs. 5 and 6). This is supported by the observation that raising extracellular K^+ from 3 to 99 mM did not increase wild-type Kv1.4 conductance when pulses

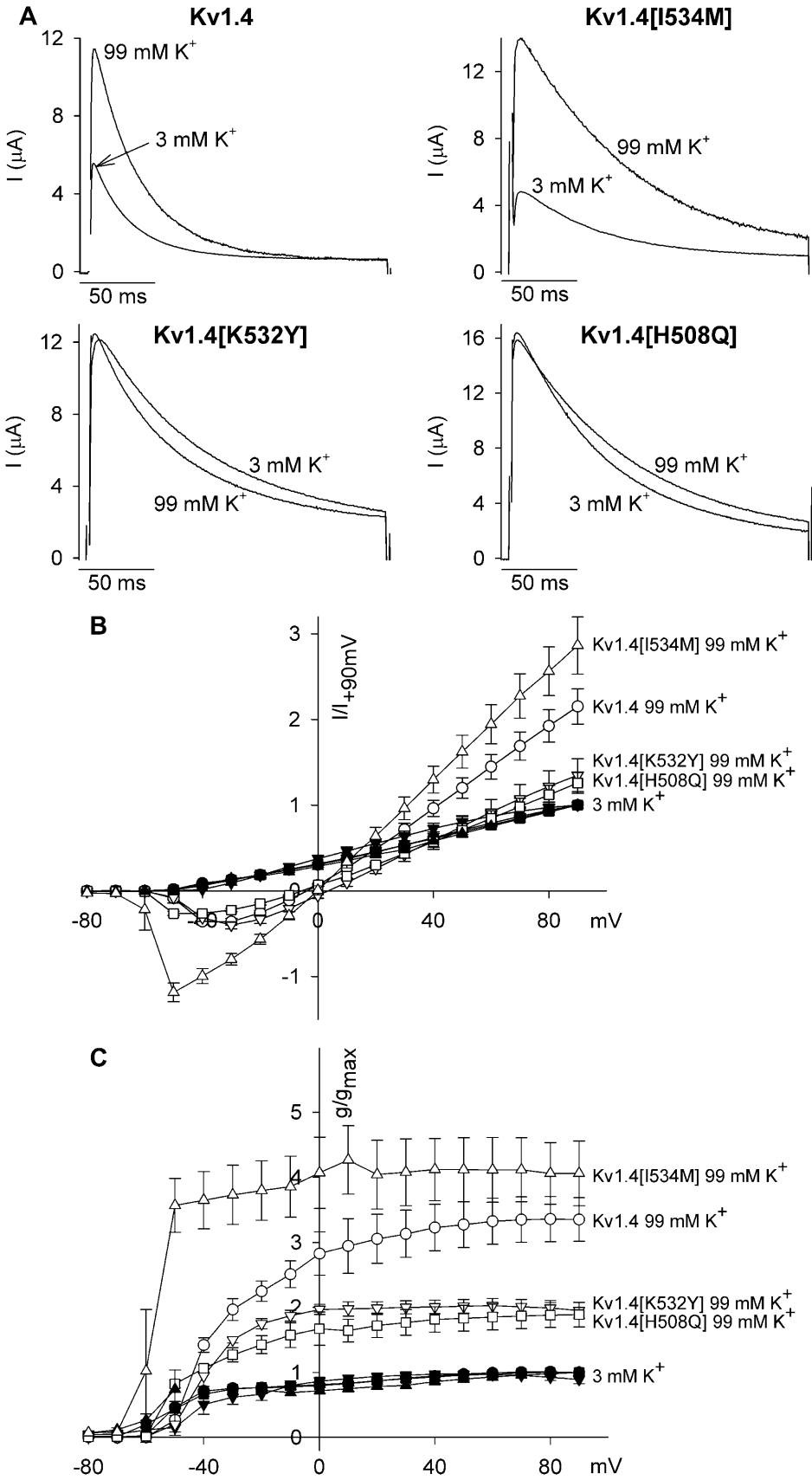

FIGURE 6 K^+ activation of wild-type and mutant Kv1.4 channels. (*A*) Typical current traces recorded during 200-ms voltage pulses to +90 mV from a holding potential of 0 mV in 3 and 99 mM extracellular K^+. (*B* and *C*) Current-voltage relationships (*B*) and conductance-voltage relationships (*C*) for each channel in 3 and 99 mM K^+. Mean ± SEM (n = 4–5) shown. Currents are normalized to the current at +90 mV in 3 mM K^+. Conductance values are normalized to the maximum conductance in 3 mM K^+.

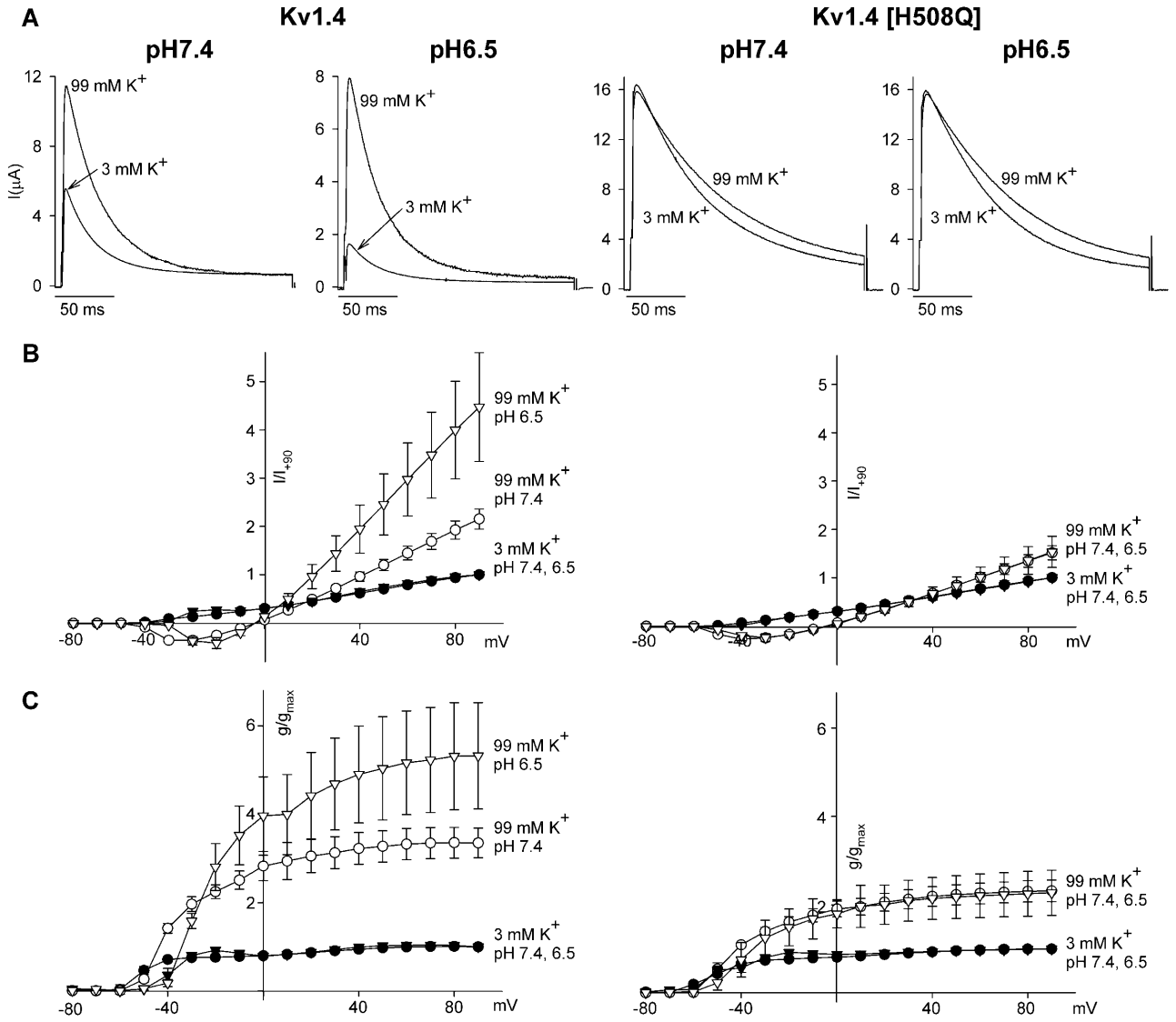

FIGURE 7 Effect of acidic pH on K^+ activation of wild-type (*left*) and H508Q mutant (*right*) Kv1.4 channels. (*A*) Typical current traces recorded during 200-ms voltage pulses to +90 mV from a holding potential of 0 mV in 3 and 99 mM K^+ at pH 7.4 and 6.5. (*B* and *C*) Current-voltage relationships (*B*) and conductance-voltage relationships (*C*) for the channels in 3 and 99 mM K^+ at pH 7.4 and 6.5. Mean ± SEM ($n = 4$–5) shown. Currents are normalized to the current at +90 mV in 3 mM K^+ at the same pH. Conductance values are normalized to the maximum conductance in 3 mM K^+ at the same pH. Data for the wild-type and H508Q mutant channels are plotted on the same scale for comparison.

were applied at an interval of 15 s, which allows for complete recovery in both 3 and 99 mM K^+ (data not shown; see also Baukrowitz and Yellen, 1995). In 3 mM K^+, recovery of the K532Y and H508Q mutant channels was faster than with the wild-type channel; τ was 791 ± 104 and 795 ± 154 ms, respectively (Fig. 8; $n = 5$–6; ANOVA, $P < 0.05$). In contrast, recovery of the I534M mutant channel and of the wild-type channel at pH 6.5 was slower than that of the wild-type channel (at pH 7.4); τ was 3125 ± 208 and 2600 ± 260 ms, respectively (Fig. 8; $n = 4$–5; ANOVA, $P < 0.05$). In Fig. 8 *B*, the increase in K^+ conductance on going from 3 to 99 mM K^+ calculated from data in Fig. 6 is plotted against the τ of recovery of wild-type and mutant channels in 3 mM K^+. The faster recovery of K532Y and H508Q mutant channels explains the reduced K^+ activation in these channels whereas the slower recovery of the I534M mutant channel and of the wild-type channel at pH 6.5 explains the enhanced K^+ activation in these channels (Fig. 8 *B*). These data show that the rate of recovery from C-type inactivation determines the extent of K^+ activation of the Kv1.4 channel.

DISCUSSION

This study has shown the importance of positively charged residues in the extracellular part of the pore of the channel in K^+ activation of the channel. The selectivity filter of the KcsA channel has been shown to collapse in low extracellular K^+ (Zhou et al., 2001; Zhou and MacKinnon,

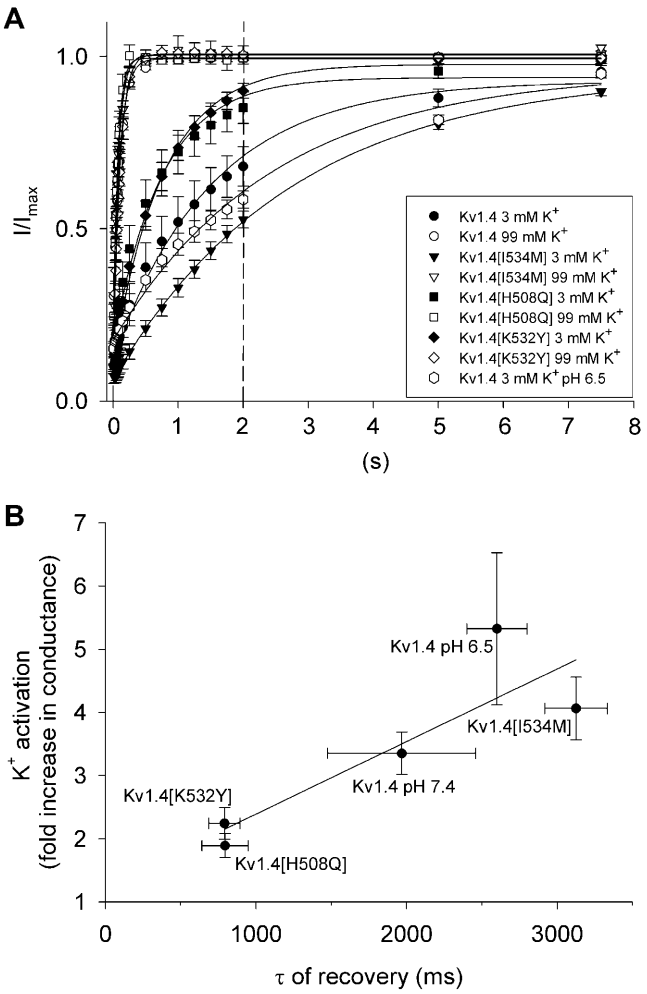

FIGURE 8 Recovery from inactivation determines K^+ activation. (*A*) Time course of recovery of wild-type and mutant Kv1.4 channels from inactivation in 3 and 99 mM extracellular K^+. Data for the recovery of the wild-type channel at pH 6.5 taken from Claydon et al. (2002) are also shown. (*B*) Correlation of the time constant, τ, of recovery from inactivation of wild-type and mutant channels in 3 mM K^+ plotted against the extent of K^+ activation. Mean ± SEM shown ($n = 4$–6).

2003). Our working hypothesis is that the selectivity filter is kept open (i.e., is kept from collapsing) when an outer coordination site in the selectivity filter (e.g., s1, the outermost K^+ coordination site within the selectivity filter) is occupied by K^+. K^+ activation is, therefore, the result of an increase in the probability of the site being occupied (the latter is the consequence of the law of mass action). This is the starting premise for the discussion below.

K^+ activation of the Kir3.1/Kir3.4 channel

We have previously shown that the salt bridge between R155 and E145 behind the selectivity filter (Fig. 1 *A*) stabilizes the selectivity filter (Dibb et al., 2003) and disruption of the salt bridge by either the R155E or E145Q mutation results in a loss of selectivity (Lancaster et al., 2000; Dibb et al., 2003). Although the R155E and E145Q mutations have similar effects on selectivity, this study has shown that the effects of the R155E and E145Q mutations differ in the case of K^+ activation and Mg^{2+} block: the R155E mutation abolished K^+ activation whereas the E145Q mutation had no effect. This suggests that the loss of K^+ activation caused by the R155 mutation is independent of the disruption of the selectivity filter caused by the mutation.

Since polyamine block is sensitive to the extracellular K^+ concentration (Lopatin and Nichols, 1996a), the effects of the mutations on K^+ activation may be the result of altered polyamine binding. Indeed, there is evidence of altered polyamine binding with the R155E and E145Q mutations. Both mutations affect the structure of the selectivity filter in such a way that extracellular polyamines can readily permeate the channel (Dibb et al., 2003). In addition, inward rectification is weakened (Dibb et al., 2003; see also Fig. 2) and the kinetics of current activation, which may be due to polyamine unbinding (Lopatin et al., 1995; Lancaster et al., 2000), are altered. The loss of the steep phase of the conductance-voltage relationships with both mutants (Fig. 2 *C*) also suggests altered polyamine binding. However, Kir2.1 channel conductance remains sensitive to extracellular K^+ even in the absence of polyamines (Lopatin and Nichols, 1996b). Furthermore, although altering extracellular K^+ shifts the conductance-voltage relationship (a reflection of polyamine block) according to the shift in the K^+ equilibrium potential (Lopatin and Nichols, 1996a), this effect cannot account for the increase in maximal conductance at higher K^+ concentrations shown in Fig. 2. Moreover, although both R155E and E145Q mutations may alter polyamine binding, only R155 mutations alter K^+ activation (Fig. 2).

We suggest that R155 is responsible for K^+ activation, because it acts as a guard to the selectivity filter and reduces the K^+ occupancy of the critical coordination site in the selectivity filter (possibly s1)—K^+ activation is the consequence of an increase in occupancy (despite R155) caused by an elevation of the extracellular K^+ concentration. In this scenario, mutation of R155 abolishes K^+ activation because occupancy is high even when the extracellular K^+ concentration is low (in other words, there is no inhibition on lowering the extracellular K^+ concentration). This conclusion is supported by the observation that the R148H mutation in the Kir2.1 channel reduces the K^+ concentration dependence of single-channel current (Shieh et al., 1999). The small effect of the E131Q mutation on K^+ activation suggests that a negative charge at this position may also influence K^+ activation as suggested for the Kir2.1 channel (Murata et al., 2002). It is interesting to note that E131 in the Kir3.1/Kir3.4 channel occupies the equivalent position to H508, which regulates K^+ activation of the Kv1.4 channel (Fig. 1 *C*). Alternatively, the E131Q mutation may alter K^+ activation allosterically by disruption of the interaction of E131 with R155.

Mg^{2+} block

Figs. 4 and 5 show that the E131Q mutation significantly reduced, but did not abolish, Mg^{2+} block of the Kir3.1/Kir3.4 channel (the mutation E131R reduced it to the same extent; data not shown). In contrast, the mutation R155E (but not R155Q) did abolish Mg^{2+} block (Figs. 4 and 5). This action cannot be the result of the salt bridge between R155 and E145, because the E145Q mutation, which also breaks the salt bridge, did not affect Mg^{2+} block (Figs. 4 and 5). The R155E mutation may alter Mg^{2+} binding at E131 allosterically by altering the interaction between R155 and E131; however, in this case, why do the E131Q and E131R mutations not abolish Mg^{2+} block as does the R155E mutation? A final possibility is that the loss of Mg^{2+} block with the R155E mutation is a consequence of the role of R155 as a guard. Perhaps the positively charged residue constitutes the energy barrier that Mg^{2+} is unable to cross.. With the loss of the barrier with the R155E mutation Mg^{2+} is now able to freely permeate the channel (this will be helped by the loss of channel selectivity with this mutation).

K^+ activation of the Kv1.4 channel

Pardo et al. (1992) previously demonstrated K^+ activation of the Kv1.4 channel. These authors showed that a double mutation of two residues in the extracellular pore, K532 and I534, abolished K^+ activation. In Fig. 6, we show that it is the K532 residue that is important, because K^+ activation was abolished by the mutation K532Y, but not by I534M. The H508Q mutation also abolished K^+ activation (Fig. 6). Both K532Y and H508Q mutations also accelerated recovery from inactivation (Fig. 8 *A*). Because recovery of wild-type and mutant Kv1.4 channels is complete at a pulse interval of 2 s in 99 mM K^+, the more complete recovery in 3 mM K^+ of K532Y and H508Q mutant channels, compared with the wild-type channel (Fig. 8 *A*), explains the reduced K^+ activation in these mutant channels. This is shown by the correlation between recovery from inactivation and K^+ activation in Fig. 8 *B*. We and others have previously shown that the K532Y and H508Q mutations also reduce the development of C-type inactivation (Rasmusson et al., 1995; Claydon et al., 2002). These data are consistent with the observation that C-type and N-type inactivation are linked with K^+ activation (Lopez-Barneo et al., 1993; Baukrowitz and Yellen, 1995) and the concept that K^+ coordination within the selectivity filter affects C-type inactivation (Lopez-Barneo et al., 1993; Ogielska and Aldrich, 1999). Therefore, whereas C-type inactivation could be a collapse of the selectivity filter and is promoted by a decrease in the K^+ occupancy of the critical coordination site in the selectivity filter, K^+ activation could be an opening of the selectivity filter as a result of an increase in the occupancy of the site. There is increasing evidence that agonist-activation of some K^+ channels may involve a gate at the selectivity filter (Claydon et al., 2003; Hommers et al., 2003; Xiao et al., 2003; Proks et al., 2003) and K^+ activation and C-type inactivation may be further examples of selectivity filter gating. It is possible that the K532Y mutation abolished K^+ activation and reduces the development of C-type inactivation as a result of an electrostatic mechanism. The model of Kv1.4 in Fig. 9 shows that the positively charged ε-amino group of K532 can be only ~4.5 Å from the center of the s1 K^+ coordination site within the selectivity filter. It is possible that K^+ at one of the outer coordination sites of the selectivity filter (e.g., s1) might experience electrostatic repulsion from the positive charge of the lysine residue. As a consequence of the K532Y mutation and the loss of the positive charge, therefore, the coordination site would be more likely to be occupied resulting in a loss of K^+ activation and a reduction of C-type inactivation. An alternative possibility is that K532 affects K^+ occupancy of the coordination site by an allosteric affect. It is possible that K532 interacts with the network of hydrogen bonds that stabilize the selectivity filter. However, given its pKa (pH 10.3), the lysine side chain is likely to be fully protonated and, therefore, unable to form a hydrogen bond. Alternatively, K532 might stabilize the selectivity filter by filling the space behind it. R155 in the Kir3.1/Kir3.4 channel may act in a similar manner.

Mutation of another extracellular charge, H508, also abolished K^+ activation of the Kv1.4 channel, suggesting that this charge also affects K^+ occupancy of the critical coordination site (Fig. 6). This is consistent with the observation that mutation of the equivalent residue, H463, in the Kv1.5 channel causes collapse of conductance in 0 mM

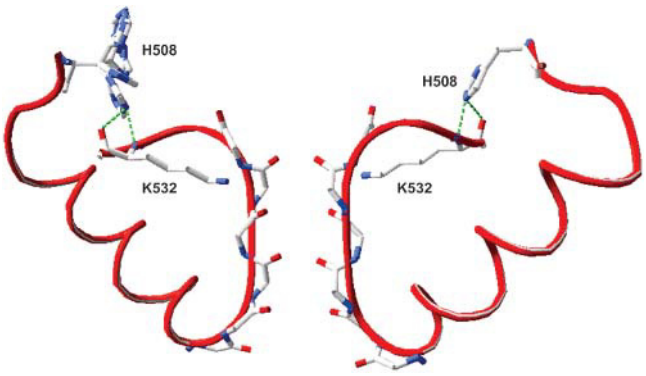

FIGURE 9 A model of the outer pore region of Kv1.4 based on the high-resolution KcsA crystal structure, 1K4C (Zhou et al., 2001), showing the K532 and H508 residues. The model was generated using Swiss-Pdb Viewer (Guex and Peitsch, 1997). Only two subunits are shown for clarity. The left-hand subunit shows a number of possible rotamers of H508. The right-hand subunit shows the ''best'' rotamer of H508. Both subunits show the ''best'' rotamer of K532. Proposed hydrogen bonds are shown by the dashed lines. The carbonyl oxygen atoms of the selectivity filter are highlighted. The position of the s1 K^+ coordination site is shown.

extracellular K^+ (Kehl et al., 2002). K^+ activation of the wild-type Kv1.4 channel was enhanced by acidic pH (Fig. 7). This is consistent with studies of the Kv1.5 channel, which show that current inhibition by acidic pH is reduced by raising extracellular K^+ (Kehl et al., 2002). In the Kv1.4 channel, the effect of pH on K^+ activation was abolished by the H508Q mutation (Fig. 7). We have previously shown that H508 in Kv1.4 acts as the pH-sensitive site mediating the effect of protons on C-type inactivation (Claydon et al., 2000, 2002). We propose that protonation of H508 increases its positive charge and this decreases K^+ occupancy of the coordination site and consequently increases C-type inactivation and K^+ activation. H508 lies near the apex of the extracellular turret at a substantial distance (~12 Å) from the selectivity filter (Fig. 9). It may affect K^+ occupancy of the coordination site as a consequence of affecting K^+ occupancy at s0 (the K^+ coordination site at the extracellular mouth of the pore) by long-range electrostatic interactions. If the four histidine residues of the tetramer are fully protonated and act as point charges, and assuming a dielectric constant of 81 (for the aqueous solution in the outer vestibule of the pore), the charge experienced at the outer K^+ coordination site was calculated to be +59 mV (2.4 RT units). Alternatively, H508 may influence K^+ occupancy at the coordination site in an indirect manner as shown in Fig. 9. The model of the left-hand subunit in Fig. 9 shows a number of different rotamers that could be formed by the H508 side chain. The ''best'' rotamer is shown in the right-hand subunit (Fig. 9). In this rotamer, the H508 side chain forms two hydrogen bonds with the backbone of the K532 residue (the hydrogen bond with the carbonyl oxygen is perhaps unfavorable given its geometry). It is possible, therefore, that manipulation of H508 could affect K^+ occupancy of the coordination site via the K532 residue (the hydrogen bonds will not exist when the histidine side chain is protonated at acidic pH). This conclusion is supported by the observation that the effects of pH involve both H508 and K532 (Claydon et al., 2002; Kehl et al., 2002). Furthermore, Wood and Korn (2000) have suggested that K^+ activation of the Kv2.1 channel involves reorganization of the extracellular pore in high K^+ such that a positive charge, K356, which is the equivalent residue to H508, is orientated toward the pore.

This study has identified residues in both an inward rectifier and a voltage-gated K^+ channel that are involved in K^+ activation. There are striking similarities in the positions of these residues in the two channel types and we suggest that there is a common mechanism of K^+ activation. Raising extracellular K^+ inhibits the collapse of the Kv1.4 channel pore as a result of C-type inactivation, suggesting that, whereas C-type inactivation is a collapse of the selectivity filter, K^+ activation is an opening of the selectivity filter. We propose that a similar inhibition of pore collapse on raising extracellular K^+ may be responsible for K^+ activation of the Kir3.1/Kir3.4 channel.

REFERENCES

Baukrowitz, T., and G. Yellen. 1995. Modulation of K^+ current by frequency and external $[K^+]$: a tale of two inactivation mechanisms. *Neuron.* 15:951–960.

Claydon, T. W., M. R. Boyett, A. Sivaprasadarao, K. Ishii, J. M. Owen, H. A. O'Beirne, R. Leach, K. Komukai, and C. H. Orchard. 2000. Inhibition of the K^+ channel Kv1.4 by acidosis: protonation of an extracellular histidine slows the recovery from N-type inactivation. *J. Physiol.* 526:253–264.

Claydon, T. W., M. R. Boyett, A. Sivaprasadarao, and C. H. Orchard. 2002. Two pore residues mediate acidosis-induced enhancement of C-type inactivation of the Kv1.4 K^+ channel. *Am. J. Physiol.* 283:C1114–C1121.

Claydon, T. W., S. Y. Makary, K. M. Dibb, and M. R. Boyett. 2003. The selectivity filter may act as the agonist-activated gate in the G protein-activated Kir3.1/Kir3.4 K^+ channel. *J. Biol. Chem.* 278:50654–50663.

Dibb, K. M., T. Rose, S. Y. Makary, T. W. Claydon, D. Enkvetchakul, R. Leach, C. G. Nichols, and M. R. Boyett. 2003. Molecular basis of ion selectivity, block and rectification of the inward rectifier Kir3.1/Kir3.4 K^+ channel. *J. Biol. Chem.* 278:49537–49548.

Doring, F., C. Derst, E. Wischmeyer, C. Karschin, R. Schneggenburger, J. Daut, and A. Karschin. 1998. The epithelial inward rectifier channel Kir7.1 displays unusual K^+ permeation properties. *J. Neurosci.* 18:8625–8636.

Guex, N., and M. C. Peitsch. 1997. Swiss-model and the Swiss-PdbViewer: An environment for comparative protein modeling. *Electrophoresis.* 18:2714–2723.

Hommers, L. G., M. J. Lohse, and M. Bunemann. 2003. Regulation of the inward rectifying properties of G-protein-activated inwardly rectifying K^+ (GIRK) channels by $G\beta\gamma$ subunits. *J. Biol. Chem.* 278:1037–1043.

Kehl, S. J., C. Eduljee, D. C. Kwan, S. Zhang, and D. Fedida. 2002. Molecular determinants of the inhibition of human Kv1.5 potassium currents by external protons and Zn^{2+}. *J. Physiol.* 541:9–24.

Kubo, Y. 1996. Effects of extracellular cations and mutations in the pore region on the inward rectifier K^+ channel IRK1. *Receptors Channels.* 4:73–83.

Lancaster, M. K., K. M. Dibb, C. C. Quinn, R. Leach, J. K. Lee, J. B. Findlay, and M. R. Boyett. 2000. Residues and mechanisms for slow activation and Ba^{2+} block of the cardiac muscarinic K^+ channel, Kir3.1/Kir3.4. *J. Biol. Chem.* 275:35831–35839.

Lopatin, A. N., E. N. Makhina, and C. G. Nichols. 1995. The mechanism of inward rectification of potassium channels: ''Long-pore plugging'' by cytoplasmic polyamines. *J. Gen. Physiol.* 106:923–955.

Lopatin, A. N., and C. G. Nichols. 1996a. $[K^+]$ dependence of polyamine-induced rectification in inward rectifier potassium channels (IRK1, Kir2.1). *J. Gen. Physiol.* 108:105–113.

Lopatin, A. N., and C. G. Nichols. 1996b. $[K^+]$ dependence of open-channel conductance in cloned inward rectificer potassium channels (IRK1, Kir2.1). *Biophys. J.* 71:682–694.

Lopez-Barneo, J., T. Hoshi, S. H. Heinemann, and R. W. Aldrich. 1993. Effects of external cations and mutations in the pore region on C-type inactivation of *Shaker* potassium channels. *Receptors Channels.* 1:61–71.

McAllister, R. E., and D. Noble. 1966. The time and voltage dependence of the slow outward current in cardiac Purkinje fibres. *J. Physiol.* 186:632–662.

Murata, Y., Y. Fujiwara, and Y. Kubo. 2002. Identification of a site involved in the block by extracellular Mg^{2+} and Ba^{2+} as well as permeation of K^+ in the Kir2.1 K^+ channel. *J. Physiol.* 544:665–677.

Ogielska, E. M., and R. W. Aldrich. 1999. Functional consequences of a decreased potassium affinity in a potassium pore. Ion interactions and C-type inactivation. *J. Gen. Physiol.* 113:347–358.

Pardo, L. A., S. H. Heinemann, H. Terlau, U. Ludewig, C. Lorra, O. Pongs, and W. Stuhmer. 1992. Extracellular K^+ specifically modulates a rat brain K^+ channel. *Proc. Natl. Acad. Sci. USA.* 89:2466–2470.

Proks, P., J. F. Antcliff, and F. M. Ashcroft. 2003. The ligand-sensitive gate of a potassium channel lies close to the selectivity filter. *EMBO Rep.* 4:70–75.

Rasmusson, R. L., M. J. Morales, R. C. Castellino, Y. Zhang, D. L. Campbell, and H. C. Strauss. 1995. C-type inactivation controls recovery in a fast inactivating cardiac K^+ channel (Kv1.4) expressed in *Xenopus* oocytes. *J. Physiol.* 489:709–721.

Shieh, R.-C., J.-C. Chang, and C.-C. Kuo. 1999. K^+ binding sites and interactions between permeating K^+ ions at the external pore mouth of an inward rectifier K^+ channel (Kir2.1). *J. Biol. Chem.* 274:17424–17430.

Wischmeyer, E., F. Doring, and A. Karschin. 2000. Stable cation coordination at a single outer pore residue defines permeation properties in Kir channels. *FEBS Lett.* 466:115–120.

Wood, M. J., and S. J. Korn. 2000. Two mechanisms of K^+-dependent potentiation in Kv2.1 potassium channels. *Biophys. J.* 79:2535–2546.

Xiao, J., X. G. Zhen, and J. Yang. 2003. Localization of PIP2 activation gate in inward rectifier K^+ channels. *Nat. Neurosci.* 6:811–818.

Yang, J., M. Yu, Y. N. Jan, and L. Y. Jan. 1997. Stabilization of ion selectivity filter by pore loop ion pairs in an inwardly rectifying potassium channel. *Proc. Natl. Acad. Sci. USA.* 94:1568–1572.

Zhou, Y., and R. MacKinnon. 2003. The occupancy of ions in the K^+ selectivity filter: charge balance and coupling of ion binding to a protein conformational change underlie high conduction rates. *J. Mol. Biol.* 333:965–975.

Zhou, Y., J. H. Morais-Cabral, A. Kaufman, and R. MacKinnon. 2001. Chemistry of ion coordination and hydration revealed by a K^+ channel-Fab complex at 2.0 Å resolution. *Nature.* 414:43–48.

Zobel, C., H. C. Cho, T. T. Nguyen, R. Pekhletski, R. J. Diaz, G. J. Wilson, and P. H. Backx. 2003. Molecular dissection of the inward rectifier potassium current (I_{K1}) in rabbit cardiomyocytes: evidence for heteromeric co-assembly of Kir2.1 and Kir2.2. *J. Physiol.* 550:365–372.